

# Electronic Structure of Low-Spin Ferric Porphyrins: Single-Crystal EPR Evidence for Pseudo-Jahn–Teller Distortion in (Tetraphenylporphinato)iron(III) Bis(imidazole) Cations

S. Michael Soltis and Charles E. Strouse\*

Contribution from the Department of Chemistry and Biochemistry, the J. D. McCullough X-ray Crystallography Laboratory, and the Solid State Science Center, University of California, Los Angeles, California 90024. Received June 15, 1987

**Abstract:** Single-crystal electron paramagnetic resonance measurements have yielded  $g$  tensors for two conformers of the (tetraphenylporphinato)iron(III) bis(imidazole) cation. Crystal field parameters derived from these  $g$  tensors, along with similar data previously obtained for three other closely related complexes, provide the basis for a thorough analysis of imidazole-mediated influences on the electronic structure. The fit of the observed data to a quantitative model of the crystal field supports the hypothesis that “pseudo-Jahn–Teller” distortion of the porphyrin ligand contributes significantly to the rhombic splitting. The magnitude of the distortion deduced from the spectroscopic data is consistent with that observed crystallographically. The model developed in this investigation can be applied in the analysis of EPR data for low-spin ferric heme proteins and in the prediction of crystal field energies and spin distributions in heme systems for which EPR data are not available.

The widespread occurrence of the heme group in biochemistry is a consequence of its unusual electronic “flexibility”. In its various biological roles the heme group takes on a wide range of oxidation states and spin states. Drastic changes in the electronic structure of this molecule can be brought about by relatively minor perturbations of its environment. In this sense, the heme acts as a chemical “amplifier”.

The routes whereby external factors influence the electronic structure of the heme have been subject to numerous investigations. Because of the common occurrence of a histidyl imidazole as an axial ligand in heme proteins, the imidazole-mediated influences on the electronic structure have been of special interest. Investigations based on structural, spectroscopic, and electrochemical measurements have been used to probe the influence of imidazole substituents, hydrogen bonding, and orientation.<sup>1–8</sup> In a recent report<sup>1</sup> from this laboratory, single-crystal and polycrystalline electron paramagnetic resonance (EPR) results from a series of five imidazole complexes revealed a systematic variation in the crystal field energies with axial ligand orientation which was attributed to a distortion of the porphyrin. This variation was correlated with observed changes in the asymmetry of the Fe–N(porphyrin) bond distances. These observations suggested that it might be possible to develop a quantitative model of the crystal field that could be applied both to the interpretation of EPR of porphyrin systems and to the prediction of electronic structure in the absence of EPR data. In the investigation reported herein, additional single-crystal EPR data have been obtained to provide the basis for such a model, a model has been developed, and various implications of the model have been explored.

## Experimental Section

Crystals of  $[\text{FeTPP}(\text{ImH})_2]\text{Cl}\cdot\text{CHCl}_3\cdot\text{H}_2\text{O}^9$  suitable for EPR analysis were obtained by a modification of the preparation reported by Scheidt, Osvath, and Lee.<sup>2</sup> A solution containing 36 mg of  $\text{Fe}(\text{TPP})\text{Cl}$  (Mid-century) and 22 mg of imidazole (Sigma, used as received) in approximately 4 mL of chloroform was layered with 4 mL of a 2:1 chloroform/hexane mixture. Crystals were obtained overnight.

**Single-Crystal EPR Measurements.** Equipment and methods used in the  $g$  tensor determination were similar to those reported previously.<sup>1,10,11</sup> All EPR measurements were made at 86 K; X-ray alignments were carried out at room temperature. In all,  $g$  values were measured as a function of rotation about five different axes. Principal  $g$  values and corresponding crystal field parameters were extracted from four combinations of three rotations (see Table I). In each combination the rotation axes were nearly orthogonal. Assignment of the two EPR signals to the two crystallographically independent complex ions was made on the basis of the angle between the largest principal axes of the  $g$  tensors and the normals to the two porphyrin ligands.

Multiple-temperature X-ray measurements indicate the presence of a phase transition in this material at about 200 K which results in an irreversible splitting of the diffraction maxima upon cooling. Splitting was also observed in the EPR spectra for particular orientations of the crystal in the magnetic field. In fitting the observed  $g$  values as a function of rotation, those orientations that gave split peaks were omitted. In the absence of a structural characterization of the low-temperature phase, particular caution must be exercised in the interpretation of the spectroscopic data.

## EPR Spectroscopy of Ferric Porphyrin Complexes

Much of the present knowledge of the electronic structure of the heme moiety is based on electron paramagnetic resonance spectroscopy. For low-spin Fe(III) species, the principal  $g$  values, readily obtained from the spectra of polycrystalline or frozen solution samples, yield the relative energies of the three iron  $d^5$  orbitals. Figure 1 contains a representation of a centrosymmetric bis(imidazole) ferric porphyrin complex, an energy level diagram of the frontier orbitals for the system, and the relationship between the principal  $g$  values and the crystal field parameters as derived

(1) Quinn, R.; Valentine, J. S.; Byrn, M. P.; Strouse, C. E. *J. Am. Chem. Soc.* **1987**, *109*, 3301.

(2) Scheidt, W. R.; Osvath, S. R.; Lee, Y. J. *J. Am. Chem. Soc.* **1987**, *109*, 1958.

(3) Scheidt, W. R.; Kirner, J. F.; Hoard, J. L.; Reed, C. A. *J. Am. Chem. Soc.* **1987**, *109*, 1963.

(4) Scheidt, W. R.; Chipman, D. M. *J. Am. Chem. Soc.* **1986**, *108*, 1163.

(5) Walker, F. A.; Huynh, B. H.; Scheidt, W. R.; Osvath, S. R. *J. Am. Chem. Soc.* **1986**, *108*, 5288.

(6) Walker, F. A.; Reis, D.; Balke, V. L. *J. Am. Chem. Soc.* **1984**, *106*, 6888.

(7) Quinn, R.; Strouse, C. E.; Valentine, J. S. *Inorg. Chem.* **1983**, *22*, 3934.

(8) Quinn, R.; Nappa, M.; Valentine, J. S. *J. Am. Chem. Soc.* **1982**, *104*, 2588.

(9) Abbreviations: TPP, tetraphenylporphinato; OEP, octaethylporphinato; TpiVPP, tetrakis(pivalamidophenyl)porphinato; PPIX, protoporphyrin IX; ImH, imidazole; cMU, *cis*-methyl urocanate; tMU, *trans*-methyl urocanate; 1MeIm, 2MeImH, and 4MeImH, 1-, 2-, and 4-methylimidazole, respectively; BMS, benzyl methyl sulfide; BeS, benzenethiolate; THT, tetrahydrothiophene; 4Mepip, 4-methylpiperidine.

(10) Byrn, M. B.; Katz, B. A.; Keder, N. L.; Levan, K. R.; Magurany, C. J.; Miller, K. M.; Pritt, J. W.; Strouse, C. E. *J. Am. Chem. Soc.* **1983**, *105*, 4916.

(11) Byrn, M. P.; Strouse, C. E. *J. Magn. Reson.* **1983**, *53*, 32.

**Table I.** Structural and Electronic Information for Centrosymmetric Imidazole Complexes of Fe<sup>III</sup>TPP

compd <sup>a</sup>	$\phi^b$	$\theta^c$	$g_1$	$g_2$	$g_3$	$\Delta/\lambda^d$	$V/\lambda$	$V/\Delta$	$\Delta\text{Fe-N}_p$	$\text{Fe-N}_a$	H bond
ImH	5	-3	1.551 (9)	2.313 (3)	2.916 (3)	3.13 (3)	1.99 (2)	0.637 (5)	0.017	1.977 (3)	2.774 (4)
cMU	15	11	1.486 (11)	2.298 (10)	2.965 (13)	3.02 (8)	1.84 (3)	0.609 (18)	0.024	1.979 (7)	2.727 (11)
tMU	22		1.471	2.269	2.964	3.095	1.801	0.582	0.007	1.983 (4)	2.801 (5)
cMU	29	28	1.481 (18)	2.265 (9)	2.999 (10)	3.22 (9)	1.77 (3)	0.551 (14)	0.002	1.967 (7)	2.614 (11)
ImH	41	42	1.480 (8)	2.271 (14)	2.988 (1)	3.17 (11)	1.789 (3)	0.566 (19)	0.005	1.964 (3)	3.035 (4)

<sup>a</sup>See ref 9 for abbreviations. <sup>b</sup>Angle measured between an Fe-N vector of the porphyrin ligand and the intersection between the plane of the axial ligand and the porphyrin plane. See Figure 2. <sup>c</sup>Angle measured between the smallest principal axis of the  $g$  tensor as projected in the plane of the porphyrin ligand and the same Fe-N vector as above. See text. <sup>d</sup>Coefficients from Taylor's analysis of the crystal field parameters yield normalizations of 1.01 for all complexes listed.

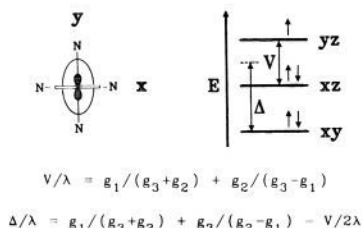


**Figure 1.** Orientations of the partially filled d orbital and the principal axes of the  $g$  tensor for a bis(imidazole) complex of Fe<sup>III</sup>TPP with the imidazole ligands eclipsing the porphyrin nitrogen atoms. The expressions for the crystal field parameters in terms of the principal  $g$  values are those derived by Taylor.<sup>12</sup> In this high-symmetry limit the principal axes of the  $g$  tensor (1, 2, and 3) correspond to the molecular axes ( $x$ ,  $y$ , and  $z$ ).

by Taylor.<sup>12</sup> Because the energies of the orbitals are strongly influenced by the axial ligation, EPR spectroscopy has been used to great profit in the study of both heme proteins and small-molecule ferric porphyrins.

Single-crystal EPR spectroscopy can provide wave functions as well as energies for the  $d^x$  orbitals, thus producing a very detailed picture of the electronic structure. Single-crystal measurements can also be used to advantage for those systems in which, because of large line widths and/or overlapping signals, the polycrystalline spectrum does not provide reliable data.

While there is a simple relationship between the orientation of the principal axes of the  $g$  tensor and the wave functions of the  $d^x$  orbitals in these porphyrin complexes, the relationship is rather counterintuitive. As predicted by Oosterhuis and Lang<sup>13</sup> and demonstrated in several investigations from this laboratory,<sup>1,10</sup> a rotation of the axial ligands about the porphyrin normal (usually expressed in terms of the angle  $\phi$ ) results in a *retrograde* rotation of the principal axes of the  $g$  tensor about the same axis.

Rotation of the axial ligands alone is not expected to result in any change in the crystal field energies, but in the previous paper in this series<sup>1</sup> a systematic decrease in the rhombic splitting,  $V$ , was observed as imidazole ligands were rotated away from the orientation in which they eclipse an Fe-N vector of the porphyrin ( $\phi = 0$ ). This change was attributed to a distortion of the porphyrin that is maximized in the eclipsed orientation. In the following sections the factors influencing the energies of the  $d^x$  orbitals are incorporated into a quantitative model for the observed  $\phi$  dependence of the rhombic splitting.

### The Frontier Orbitals of Ferric Porphyrin Complexes

Several factors of comparable magnitude interact to determine the nature and energy of the highest occupied molecular orbitals of ferric porphyrin complexes. These include crystal field, spin-orbit, and vibronic effects. In the absence of axial ligands and spin-orbit coupling, the Fe(III) complexes of symmetric porphyrins are Jahn-Teller active. The spin is distributed equally over the two out-of-plane real d orbitals, but the complex is unstable with respect to distortions that tend to localize the spin, increase the rhombic splitting, and reduce the overall energy. Introduction of asymmetric axial ligands lowers the symmetry of the crystal

field, stabilizes one of the two orthogonal d orbitals with respect to the other, and localizes the spin.

In the limit where the contribution of the axial ligands to the rhombic splitting is small compared to the Jahn-Teller stabilization energy, the effect of the axial ligands is amplified;<sup>14</sup> i.e., the magnitude of the observed distortion is governed by Jahn-Teller considerations. In such a "pseudo-Jahn-Teller" system, the effects of vibronic interactions are manifest in both an observable distortion and a "softening" of the vibrational mode associated with the distortion. In the limit where the rhombic splitting from the axial ligands is large compared to the Jahn-Teller stabilization energy, the spin will be completely localized and vibronic effects will be "quenched". There will, however, be an observable distortion of the porphyrin caused by the unequal occupancy of the two d orbitals, and this distortion will contribute to the rhombic splitting. This is a pseudo-Jahn-Teller effect in the sense that the distortion is driven by unequal occupancies of the out-of-plane d orbitals and in the sense that the magnitude of the distortion is to first order independent of the magnitude of the perturbation. Since, however, vibronic mixing is not significant in this limit, this is not a pseudo-Jahn-Teller effect in the usual sense of the term. In cases where the Jahn-Teller stabilization energy is comparable to the crystal field splitting produced by the axial ligands, this distinction disappears.

Spin-orbit coupling must also be considered in these systems. This interaction tends to stabilize a delocalized ground state; i.e., the eigenfunctions of the spin-orbit Hamiltonian contain equal contributions from the two real d orbitals. In the limit where the spin-orbit coupling constant is large compared to the crystal field splitting, all Jahn-Teller or pseudo-Jahn-Teller effects (vibronic or otherwise) will be quenched. There will be no distortion and no mode softening.

In keeping with an overall pattern of "electronic flexibility" in iron porphyrin systems, most ferric porphyrin complexes do not approach any of the limits discussed above. For these complexes it appears that the Jahn-Teller stabilization energy, the spin-orbit coupling constant, the rhombic splitting associated with typical axial ligands, and the zero-point energy of potential distortional modes are all on the order of hundreds of wavenumbers. This, of course, complicates the analysis of the electronic structure; one must be careful to consider crystal field, vibronic, and spin-orbit effects in each individual case.

For centrosymmetric bis(imidazole) complexes of Fe<sup>III</sup>TPP, the observed rhombic crystal field splitting is approximately twice the spin-orbit coupling constant. Experimental observations suggest that the maximum contribution to the rhombic splitting that results from distortion of the porphyrin is on the order of half the spin-orbit coupling constant (vide infra). The following analysis of this system begins with a fully localized description. Spin-orbit effects are treated explicitly in determination of the crystal field parameters. Vibronic effects are included in the analysis to the extent that they contribute to the distortion of the porphyrin.

### $\phi$ Dependence of the Rhombic Splitting

**Axial Ligand Contribution.** In the following,  $\theta$  is defined as the angle between the symmetry axis of the partially filled orbital and one of the Fe-N vectors of the porphyrin. For an idealized

(12) Taylor, C. P. S. *Biochim. Biophys. Acta* **1977**, *491*, 137.

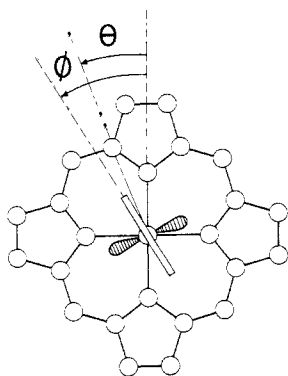
(13) Oosterhuis, W. T.; Lang, G. *Phys. Rev.* **1969**, *178*, 439.

(14) Bersuker, I. B. In *The Jahn-Teller Effect and Vibronic Interactions in Modern Chemistry*; Plenum: New York, 1984; pp 180.

**Table II.** Structural Parameters for Bis Axial Ligand Iron(III) Porphyrin Complexes

axial ligands <sup>a</sup>	$\phi^b$	$\phi_{ave}$	Fe-N(A) <sup>c</sup>	Fe-N(B) <sup>d</sup>	A-B	ref
Cationic Complexes						
ImH	5	5	2.002 (3)	1.985 (3)	0.017	<i>e</i>
1MeIm	3, 16	10	2.002 (5)	1.979 (6)	0.023	<i>f</i>
cMU	15	15	2.007 (7)	1.983 (7)	0.024	<i>g</i>
BMS	5, 35	20	1.984 (5)	1.977 (5)	0.007	<i>h</i>
tMU	22	22	1.995 (4)	1.988 (4)	0.007	<i>g</i>
THT	26	26	1.985 (3)	1.986 (3)	-0.001	<i>i</i>
cMU	29	29	1.998 (7)	1.996 (7)	0.002	<i>g</i>
THT	34	34	1.980 (3)	1.989 (3)	-0.009	<i>i</i>
ImH	41	41	1.995 (3)	1.990 (3)	0.005	<i>e</i>
Anionic Complexes						
BeS	4	4	2.013 (4)	2.003 (4)	-0.010	<i>j</i>
4MeIm	-1, 17	8	2.018 (11)	1.978 (12)	-0.040	<i>k</i>

<sup>a</sup>See ref 9 for abbreviations. Complexes having  $\phi_1 - \phi_2 \cong 90^\circ$  have been omitted since in this limit the unpaired electron may be delocalized over the two out-of-plane d orbitals (ref 16). All complexes except the one containing 1MeIm have equatorial TPP ligands. The complex containing 1MeIm has an equatorial PPIX ligand. <sup>b</sup>Defined as in Figure 2. <sup>c</sup>Bond length of the Fe-N vector of the porphyrin most nearly aligned with the axial ligand plane (imidazole complexes) or pseudosymmetry plane normal (thioether complexes). <sup>d</sup>Bond length of the Fe-N vector of the porphyrin ligand perpendicular to the Fe-N(A) vector. <sup>e</sup>Reference 2. <sup>f</sup>Little, R. G.; Dymock, K. R.; Ibers, J. A. *J. Am. Chem. Soc.* **1975**, *97*, 4532. <sup>g</sup>Reference 1. <sup>h</sup>Soltis, S. M.; Strouse, C. F., to be published. <sup>i</sup>Mashiko, T.; Reed, C. A.; Haller, K. J.; Kastner, M. E.; Scheidt, W. R. *J. Am. Chem. Soc.* **1981**, *103*, 5758. <sup>j</sup>Reference 10. <sup>k</sup>Reference 7.

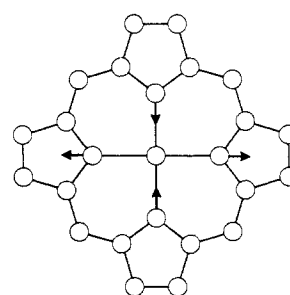


**Figure 2.** Definitions of  $\theta$  and  $\phi$ . For an idealized complex, the angle  $\theta$  is defined as the angle between the symmetry axis of the half-filled orbital and the closest Fe-N(pyrrole) vector. The magnitude of  $\theta$  is determined experimentally as the angle between the projection of the smallest principal axis of the  $g$  tensor in the plane of the porphyrin and the nearest Fe-N vector (see text). For imidazole ligands  $\phi$  is defined as the angle between the same Fe-N vector and the intersection of the plane of the axial ligand and the plane of the porphyrin ligand. In the case of thioether ligands,  $\phi$  is taken as the angle between the projection of the normal to the pseudosymmetry plane of the axial ligand and the Fe-N vector (see text).

imidazole complex,  $\phi_L$  is defined as the angle between the plane of the axial ligands and the same Fe-N vector (see Figure 2). With these definitions the angular dependence of the contribution of the axial ligand to the rhombic splitting can be expressed as  $V_L^\circ \cos 2(\theta - \phi_L)$ , where the parameter  $V_L^\circ$  is characteristic of the ligand.

Data presented in an earlier paper<sup>10</sup> showed that for complexes with the same donor atom, the same hybridization, and approximately the same ligand orientation,  $V$  and  $\Delta$  appear to scale in the same way as a function of the  $\sigma$ -donor strength of the axial ligands. That is, plots of  $V$  vs  $\Delta$  for similar ligands are approximately linear with zero intercept. The rhombicity,  $V/\Delta$ , is thus a measure of the "intrinsic asymmetry" of the donor atom and is little affected by changes in the axial ligand remote from the donor atom. This observation was rationalized in terms similar to those used in angular overlap calculations. On the basis of this observation, the utility of the above expression for the ligand contribution to the rhombic splitting can be increased by replacing the parameter  $V_L^\circ$  with the product of a rhombicity parameter,  $(V/\Delta)_L^\circ$ , and the observed  $\Delta$  to give  $(V/\Delta)_L^\circ \Delta_{obsd} \cos 2(\theta - \phi_L)$  for the ligand contribution to  $V$ .

**"Pseudo-Jahn-Teller" Contribution.** If the magnitude of a distortion of the porphyrin ligand is represented by  $Q$ , the contribution of this distortion to the rhombic splitting can be approximated as  $Q(dV/dQ)$ . The decrease in energy of a  $d^5$  complex

**Figure 3.** Representation of the  $b_{1g}$  distortion of a porphyrin ligand.

resulting from the increase in rhombic splitting,  $-1/2 Q(dV/dQ)$ , is countered by a  $1/2 f Q^2$  energy gain, where  $f$  is the force constant associated with the distortional mode. Setting  $dE/dQ = 0$  requires that  $Q = (dV/dQ)/2f$  and results in a contribution to the rhombic splitting of  $(dV/dQ)^2/2f$ . Under  $D_{4h}$  the porphyrin is unstable with respect to distortions of  $b_{1g}$  and  $b_{2g}$  symmetry.<sup>15</sup> A  $b_{1g}$  distortion of the type represented in Figure 3 would be expected to have a large value of  $dV/dQ$  and hence be the most significant contributor to the rhombic splitting.

For the general case in which the  $\phi$  of the axial ligands is not zero, the contribution of a  $b_{1g}$  distortion to the rhombic splitting can be written as  $Q(dV/dQ)^\circ \cos \theta$ . The resulting distortion,  $Q = (dV/dQ)^\circ \cos \theta / 2f$ , produces a rhombic splitting of  $V_J^\circ \cos^2 \theta$ , where  $V_J^\circ = ((dV/dQ)^\circ)^2 / 2f$ .

One effect of the porphyrin distortion in centrosymmetric complexes is to make the observed  $\theta$  less than the  $\phi$  associated with the axial ligands. The constraint that  $dE/d\theta = 0$  can be used to predict the  $\theta$  for the half-filled orbital. The final expressions for the rhombic splitting and the derivative of the energy with respect to  $\theta$  are as follows:

$$V = (V/\Delta)_L^\circ \Delta \cos 2(\theta - \phi) + V_J^\circ \cos^2 2\theta$$

and

$$dE/d\theta = (V/\Delta)_L^\circ \Delta \sin 2(\theta - \phi) + V_J^\circ \cos 2\theta \sin 2\theta = 0$$

It should be noted that any lattice-induced distortion of the porphyrin ligand will also contribute to the rhombic splitting. On the basis of structure determinations of a number of low-spin ferric TPP and OEP complexes, it appears that for small  $\phi$ , the magnitude of the pseudo-Jahn-Teller distortion usually exceeds these lattice-induced distortions. That is, in eight of nine cationic low-spin ferric porphyrin complexes for which structural data are available (see Table II), the Fe-N<sub>p</sub> distances most nearly aligned with the plane of the half-filled orbital are less than or essentially

(15) Hoffman, B. M.; Ratner, M. A. *Mol. Phys.* **1978**, *35*, 901.

**Table III.** Structural Parameters for Bis Axial Ligand Iron(II) Porphyrin Complexes

axial ligands	$\phi^b$	$\phi_{ave}$	Fe-N(A) <sup>c</sup>	Fe-N(B) <sup>d</sup>	A-B	ref
(ImH)(THT)	1, 14	7	2.994 (5)	2.988 (5)	0.006	<i>e</i>
(THT) <sub>2</sub> -A	12	12	1.992 (6)	2.003 (6)	-0.011	<i>e</i>
(THT) <sub>2</sub> -B	17	17	1.999 (6)	1.990 (6)	0.009	<i>e</i>
(2MeImH) <sub>2</sub>	22	22	2.068 (5)	2.075 (5)	-0.007	<i>f</i>
(ImH)(O <sub>2</sub> ) <sup>g</sup>	25	25	2.013 (4)	2.003 (4)	-0.010	<i>h</i>
(Pip)(NO)-B	37, -15	26	2.001 (9)	2.009 (9)	0.008	<i>i</i>
(Pip)(NO)-A	20, 43	31	2.001 (6)	1.996 (7)	0.005	<i>i</i>
(Py) <sub>2</sub>	35	35	1.997 (1)	1.989 (1)	0.008	<i>j</i>
(Py)(CO)	45	45	2.01 (1)	2.03 (1)	-0.02	<i>k</i>

<sup>a</sup> See ref 9 for abbreviations. All complexes except the one containing 2MeImH have equatorial TPP ligands. The complex containing 2MeImH has an equatorial TpvPP ligand. <sup>b</sup> Defined as in Figure 2. <sup>c</sup> Bond length of the Fe-N vector of the porphyrin most nearly aligned with the normal to the axial ligand plane (imidazole, pyridine, piperidine, NO) or pseudosymmetry plane normal (thioether). <sup>d</sup> Bond length of Fe-N vector of the porphyrin ligand perpendicular to the Fe-N(A) vector of the porphyrin ligand. <sup>e</sup> Mashiko, T.; Reed, C. A.; Haller, K. J.; Kastner, M. E.; Scheidt, W. R. *J. Am. Chem. Soc.* **1981**, *103*, 5758. <sup>f</sup> Jameson, G. B.; Molinaro, F. S.; Ibers, J. A.; Collman, J. P. *J. Am. Chem. Soc.* **1978**, *102*, 3224. <sup>g</sup> The O<sub>2</sub> ligand is disordered about the porphyrin normal by 90°. <sup>h</sup> Scheidt, W. R.; Piccolo, P. L. *J. Am. Chem. Soc.* **1976**, *98*, 1913. <sup>i</sup> Scheidt, W. R.; Brinegar, A. C.; Ferro, E. B.; Kirner, F. K. *J. Am. Chem. Soc.* **1977**, *99*, 7315. <sup>j</sup> Li, B. N.; Petricek, V.; Coppens, P. *Acta Crystallogr., Sect C* **1985**, *41*, 902. <sup>k</sup> Peng, S.; Ibers, J. A. *J. Am. Chem. Soc.* **1976**, *98*, 8032.

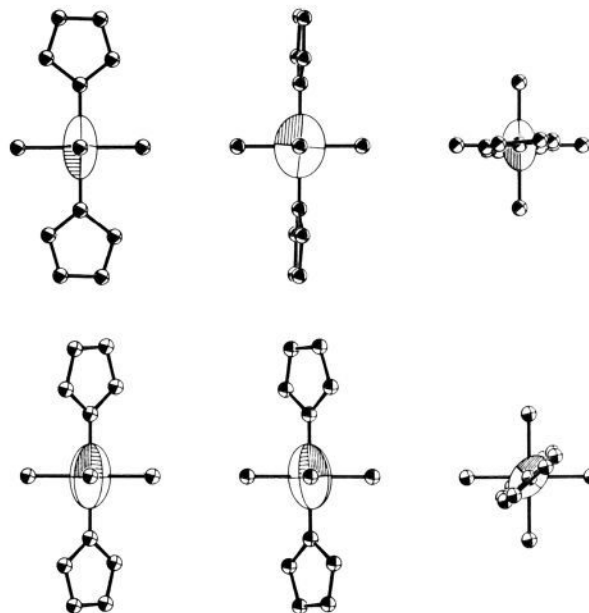
equal to those more nearly perpendicular to the plane of the half-filled orbital. Since in any individual case, however, the differences observed are small and at best marginally significant, it is difficult to judge the typical magnitude of lattice-induced distortions. For the two anionic complexes in Table II, the relative lengths of the Fe-N(porphyrin) distances are reversed. This observation will be explored in future investigations. A similar compilation of bond distances for iron(II) porphyrin complexes is given in Table III. In all cases the differences in the bond distances are small and the signs of the differences appear to be random.

### Results and Discussion

The five complexes discussed herein were chosen for study because they cover nearly the full range of imidazole ligand orientation. The analysis is simplified by the fact that all five of these complexes are centrosymmetric. Three of the complexes contain substituted imidazole ligands, cis and trans isomers of methyl urocinate (cMU and tMU, respectively). Structural data for two conformers of the Fe<sup>III</sup>TPP(cMU)<sub>2</sub> cation,  $\phi = 15$  and  $29^\circ$ , and for one conformer of the Fe<sup>III</sup>TPP(tMU)<sub>2</sub> cation,  $\phi = 22^\circ$ , were reported in an earlier paper in this series along with single-crystal EPR data for the cMU species and polycrystalline data for the tMU species. In that paper, structural and EPR data reported by Scheidt, Walker, and co-workers<sup>5</sup> were used for two conformers of the Fe<sup>III</sup>TPP(ImH)<sub>2</sub> cation,  $\phi = 5$  and  $41^\circ$ . The principal *g* values for these species were extracted from overlapping polycrystalline spectra. The single-crystal measurements reported herein were undertaken in an effort to improve the accuracy of these *g* values. Accurate values are essential to a detailed analysis of the electronic structure in this series of closely related complexes.

**Single-Crystal EPR Results.** Figure 4 provides a graphical depiction of the *g* tensors for the two conformers of the Fe<sup>III</sup>TPP(ImH)<sub>2</sub> cation. A summary of the structural and spectroscopic parameters is given in Table I, and the direction cosines of the principal axes of the *g* tensors in molecule-based coordinate systems are given in Table IV. The principal axes of the *g* tensors for the two species are approximately in the expected orientations. The principal axes corresponding to the maximum *g* values are 5 (1) and 4 (1)° from the porphyrin normals for molecules A and B, respectively. The  $\theta$ , as reflected in the angle between the Fe-N(1) vector and the projection of the *g*<sub>2</sub> axis in the porphyrin plane, is -3 (1)° for molecule A and 42 (1)° for molecule B. The corresponding crystallographic  $\phi$ , measured as the angle between the Fe-N(1) vector and the projection of the normal to the imidazole plane in the porphyrin plane, is 5° for molecule A and 41° for molecule B (see Figure 4).

**Analysis of the Crystal Field Parameters.** Figure 5 shows the  $\phi$  dependence of the rhombicity and summarizes the structural data available for these complexes. The first four complexes show a smooth variation of  $V/\Delta$  with  $\phi$ , which is consistent with the model developed above. The fifth point in Figure 5 ( $\phi = 41^\circ$ )

**Figure 4.** *g* tensor representations for two conformers of [Fe(TPP)(ImH)<sub>2</sub>]<sup>+</sup> as viewed along three molecular axes.**Table IV.** Direction Cosines<sup>a</sup> of the Principal Axes of the *g* Tensor in the Molecular Coordinate System of [Fe(TPP)(ImH)<sub>2</sub>]<sup>+</sup><sup>b</sup>

<i>g</i> value	<i>x</i>	<i>y</i>	<i>z</i>
$\phi = 5^\circ$			
1.551	-0.99834	0.05756	-0.00524
2.313	0.05756	0.93768	-0.09411
2.916	0.00756	0.09411	0.99540
$\phi = 41^\circ$			
1.480	0.73254	-0.67816	0.06627
2.271	-0.68072	-0.73254	0.02269
2.988	0.02967	-0.06279	-0.99744

<sup>a</sup> Average values of four permutations (five data sets) in the *g* tensor analysis. <sup>b</sup> *z* is the porphyrin normal and *x* is the Fe-N(O2) vector and the Fe-N(O6) vector for  $\phi = 5^\circ$  and  $\phi = 41^\circ$  complexes, respectively, as labeled by Scheidt et al.<sup>2</sup>

differs significantly from the others. One potential source of the uniqueness of the fifth data point is the fact the imidazole ligands in this complex are hydrogen bonded to chloride ions, while in all the other complexes they are hydrogen bonded to neutral oxygen-containing species. This explanation, however, seems inconsistent with the observation that in other cases  $V$  and  $\Delta$  appear to scale in the same way with ligand substitution. There is also the possibility that the experimental measurement is being influenced in some way by the observed phase transition.

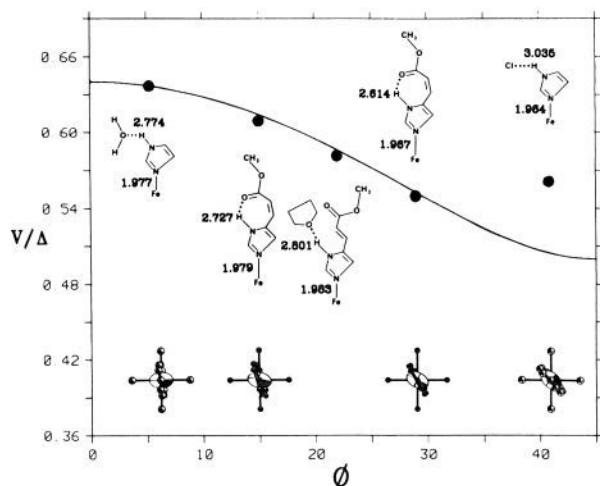


**Figure 5.**  $\phi$  dependence of the rhombicity,  $V/\Delta$ , for various Fe(TPP) bis(imidazole) complexes. The solid line represents the best fit of the experimental data to the proposed crystal field model (see text). The  $g$  tensor representations are viewed down the porphyrin normals.

**Table V.** Observed and Calculated Crystal Field Parameters<sup>a</sup>

	$\phi$				
	5	15	22	29	41
$V_{\text{obsd}}$	1.99	1.84	1.80	1.77	1.79
$V_{\text{calcd}}^b$	1.98	1.85	1.81	1.77	1.60
$\theta_{\text{obsd}}$	-3.0	11		28	42
$\theta_{\text{calcd}}^b$	3.0	12	18	25	39
$V_{\text{obsd}}/\Delta$	0.636	0.609	0.582	0.550	0.564
$V_{\text{calcd}}/\Delta^b$	0.631	0.613	0.584	0.549	0.504

<sup>a</sup>  $V$  and  $\Delta$  are in units of the spin-orbit coupling constant;  $\phi$  and  $\theta$  are expressed in degrees. <sup>b</sup> Based on a fit of the first four observations.

While no unambiguous explanation is offered for the anomalous value of  $V/\Delta$  for the  $\phi = 41^\circ$  complex, the fact that the values for the first four complexes are in good accord with the predicted behavior appears to justify an analysis that excludes the  $\phi = 41^\circ$  observation. A fit to the rhombic splitting for the first four complexes to the proposed model is summarized in Table V. This fit gave values of  $(V/\Delta)_L = 0.50$  and  $V_J = 0.42\lambda$ , where  $\lambda$  is the spin-orbit coupling constant. The solid line in Figure 5 is a calculated curve based on these parameters and an average  $\Delta = 3.1\lambda$ . In this fit, the  $\theta$  for each complex was calculated based on the constraint that  $dE/d\theta = 0$ . Comparison of these calculated  $\theta$ 's with the observed  $\theta$ 's constitutes an independent check on the validity of the model. Unfortunately, the occurrence of the phase transition in the unsubstituted material and the fact that the X-ray and EPR measurements were made at different temperatures introduce significant uncertainties in the observed  $\theta$ 's for the  $\phi = 5^\circ$  and  $\phi = 41^\circ$  complexes. This may account for the poorer correspondence between the observed and calculated  $\theta$ 's for these two complexes. The  $\phi = 15^\circ$  and  $\phi = 29^\circ$  complexes give observed  $\theta$ 's of  $11^\circ$  and  $28^\circ$ , respectively, in reasonable accord with the calculated values of  $12^\circ$  and  $25^\circ$ .

The magnitude of the pseudo-Jahn-Teller parameter,  $V_J = 0.42\lambda$ , is of significance in several respects. First this value corresponds to about half the contribution to the rhombic splitting from a single imidazole ligand; clearly this contribution cannot be neglected in any quantitative analysis of the crystal field. A second consideration is the magnitude of the pseudo-Jahn-Teller contribution with respect to the spin-orbit coupling constant. The fact that the potential Jahn-Teller stabilization is nearly half the maximum spin-orbit stabilization could result in a softness of axially symmetric systems toward lattice-induced distortions. This aspect of the electronic structure of ferric porphyrins will be addressed in detail in a future paper in this series.<sup>16</sup>

In interpreting the magnitude of  $V_J$ , one must consider to what extent the associated  $Q$  represents a nuclear as opposed to an electronic distortion. That is, does the observed change in the rhombic splitting result from a nuclear displacement, or could it rather result from a redistribution of electronic charge in the porphyrin ligand? With respect to their contribution to the  $\phi$  dependence of the  $V$ , these "distortions" might be indistinguishable. If, however, one assumes that the distortion is nuclear, one can use the vibrational force constant to predict the magnitude of the displacement, which can be compared to that observed crystallographically.

The value of the vibrational force constant,  $f$ , for the  $b_{1g}$  distortion can be estimated to be  $4K(M-N)$ , where  $K(M-N)$  is the force constant for the metal-nitrogen stretch. In a full vibrational analysis of nickel octaethylporphyrin, Abe, Kitagawa, and Kyogoku<sup>17</sup> obtained a value of  $0.7 \text{ mdyne/\AA}$  for  $K(M-N)$ . This corresponds to a displacement  $Q = (V_J/2f)^{1/2} = 0.02 \text{ \AA}$  or a difference in  $M-N$  distances of  $0.04 \text{ \AA}$ , which is on the order of the crystallographically observed differences in the limit of low  $\phi$ . This result supports the assignment of the observed  $\phi$  dependence of  $V$  to a nuclear displacement. It should be noted that the distortions observed for systems like these in which the HOMOs are of  $\pi$  symmetry are substantially smaller than those observed in  $d^9$  complexes where the degenerate orbitals are of  $\sigma$  symmetry.

On the basis of the fit described above, one can predict that in the limit of an eclipsed configuration ( $\phi = 0$ ),  $V/\Delta$  should approach a value of 0.64 (see Figure 5). Walker, Reis, and Balke<sup>6</sup> observed that frozen solutions of six different substituted imidazole complexes of Fe<sup>III</sup>TPP gave  $V/\Delta = 0.65 \pm 0.02$  (with  $\Delta$  in the range  $3.02-3.32\lambda$ ). These observations are in excellent accord with the prediction if it is assumed that in frozen solution the complexes tend to adopt a minimum energy conformation with  $\phi$  ca. 0. Scheidt and Chipman<sup>4</sup> have argued previously that the minimum energy conformation corresponds to one of low  $\phi$ , and indeed a pseudo-Jahn-Teller distortion of the porphyrin ligand contributes to the stability of this conformation.

**Fe-N(axial) Bond Distances.** Structural investigations of bis(imidazole) complexes have revealed a correlation between the axial ligand orientation,  $\phi$ , and the Fe-N(axial) bond distance.<sup>1</sup> In several complexes with two different ligand orientations, the ligand with the smaller  $\phi$  has been observed to have the larger Fe-N(axial) distance. This effect has been attributed to steric repulsion between imidazole hydrogen atoms and the porphyrin nitrogen atoms in the low- $\phi$  limit. The influence of the porphyrin distortion on the electronic structure of these complexes could provide an alternative explanation for the observations, but as Scheidt, Osvath, and Lee<sup>2</sup> were careful to point out, "the value of  $\phi$  does not appear to be a predictor of the absolute value of the axial bond length". In the two pairs of centrosymmetric conformers examined in this investigation it is again observed that the conformer with the smaller  $\phi$  has the larger bond distance, but it is difficult to rationalize the fact that the bond distance for the tMU complex with  $\phi = 22^\circ$  is longer than that of any of the others. It should be noted that for these complexes there is a good correlation between the Fe-N(axial) bond distance and the hydrogen bond N...O distance of the ligand. As would be expected, shorter Fe-N bond distances are associated with shorter N...O distances. Any effort to account for differences in Fe-N(axial) distances must certainly take into consideration differences in hydrogen bonding.

## Conclusions

Analysis of the crystal field parameters for a series of bis(imidazole) complexes of (tetraphenylporphyrinato)iron(III) obtained from EPR measurements supports the hypothesis that pseudo-Jahn-Teller distortion of the porphyrin ligand in these complexes contributes significantly to the rhombic splitting. The fit of a quantitative model of the crystal field to the experimental data indicates that the maximum contribution of the pseudo-Jahn-

(16) Inniss, D.; Soltis, S. M.; Strouse, C. E., *J. Am. Chem. Soc.*, manuscript accepted for publication.

(17) Abe, M.; Kitagawa, T.; Kyogoku, J. *Chem. Phys.* **1978**, *69*, 4526.

Teller distortion is equal to approximately half the spin-orbit coupling constant and approximately half the contribution from a single imidazole ligand. There is a reasonable correspondence between the magnitude of the porphyrin distortion deduced from the spectroscopic data and the distortions observed crystallographically. It appears that the simple model developed in this investigation could be profitably applied to the analysis of EPR data for other porphyrin and heme systems and that it could also

be used to predict crystal field energies and spin distributions in low-spin ferric porphyrin systems for which EPR data are not available.

**Acknowledgment.** We acknowledge the support of the National Institutes of Health (Grant GM35329), the National Science Foundation (Grant CHE 87-06780), and the UCLA Biomedical Research Support Grant.

## Carbon Acidity. 73. Conductimetric Study of Lithium and Cesium Salts of Hydrocarbon Acids. A Scale of Free Ion Acidities in Tetrahydrofuran. Revision of the Ion Pair Scales

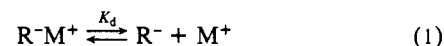
Michael J. Kaufman, Scott Gronert, and Andrew Streitwieser, Jr.\*

Contribution from the Department of Chemistry, University of California, Berkeley, California 94720. Received April 28, 1987

**Abstract:** Equilibrium constants for the dissociation of the lithium and cesium salts of eleven hydrocarbons have been determined in tetrahydrofuran solution by a conductimetric technique. The dissociation constants for the fluorenyllithium derivatives are found to be remarkably insensitive to the structure of the carbanion; this is consistent with these compounds existing as solvent separated ion pairs. The  $K_d$ 's of these lithium salts may be approximated by the primitive Bjerrum model of dissociation. The dissociation constants of the organocesium compounds are generally  $10^2$ – $10^3$  times lower than those of the corresponding lithium salts, and are consistent with the cesium compounds forming contact ion pairs. The variation of dissociation constants with molecular structure for organocesium compounds is complex, and apparently it is dependent on the charge distribution and steric bulk of the carbanion. The conductimetric dissociation constants can be used to construct a scale of relative free ion acidities in tetrahydrofuran. Comparison of the resulting ionic  $pK$  values with those measured in the ion pairing solvent dimethoxyethane and the ionizing solvent dimethyl sulfoxide reveals that the relative acidities of hydrocarbons yielding delocalized anions are almost identical in each solvent. The present data are used to revise the previously published cesium ion pair scale in THF.

Alkali metal salts of carbanions exist predominantly as ion pairs in low polarity solvents such as ethers. Through the classic work of Hogen-Esch and Schmid, it is now known that two types of thermodynamically distinct ion pairs can be identified.<sup>1-12</sup> The first type, denoted "tight" or contact ion pairs (CIP's), are characterized by relatively strong carbanion-metal interactions. Contact ion pairing is promoted by large metal ions such as cesium and by localized carbanionic charge. The second type, denoted "loose" or solvent separated ion pairs (SSIP's), have weaker carbanion-metal interactions. Solvent separated ion pairs are formed by many lithium salts of delocalized hydrocarbons in ethereal solvents. Along with ion pairs, significant concentrations of free ions are observed in ethers if the carbanion is sufficiently delocalized, and the cation is strongly coordinated to solvent (i.e., lithium salts).<sup>3,13-16</sup> Although usually less abundant, the free ions

are important in the dilute solution reactions of delocalized carbanions because they are generally more reactive.<sup>3,14,16b</sup> Solov'yanov et al.<sup>14</sup> have affirmed these conclusions with several studies comparing the abundance and reactivity of free vs ion paired lithium carbanion salts in dimethoxyethane (DME). A study from this laboratory in the following paper<sup>3a</sup> further implicates the importance of free carbanion reactions in ethereal solutions. Obviously, to fully understand the reactivity of delocalized organometallic reagents in ethers, both ion pairs and free ions must be considered and, consequently, the dissociative equilibrium that links them, eq 1.



In previous publications, we have presented scales of ion pair  $pK$  values in tetrahydrofuran (THF) for hydrocarbons of the fluorene and polyarylmethane type using both lithium<sup>17</sup> and

- (1) Hogen-Esch, T. E.; Smid, J. *J. Am. Chem. Soc.* **1965**, *87*, 669.
- (2) Hogen-Esch, T. E.; Smid, J. *J. Am. Chem. Soc.* **1966**, *88*, 307.
- (3) (a) Gronert, S.; Streitwieser, A., Jr. *J. Am. Chem. Soc.*, following paper in this issue (No. 74). (b) Gronert, S.; Streitwieser, A., Jr. *J. Am. Chem. Soc.* following in this issue (No. 75).
- (4) Karasawa, Y.; Levin, G.; Szwarc, M. *Proc. R. Soc. London A* **1971**, *326*, 53.
- (5) Petrov, E. S.; Belovsova, M. I.; Shatenshtein, A. I. *Org. React.* **1965**, *2*, 316.
- (6) Szwarc, M.; Jagur-Grotzinski, J. In *Ions and Ion Pairs in Organic Reactions*; Szwarc, M., Ed.; Wiley-Interscience: New York, 1974; Vol. 2.
- (7) Buncel, E.; Menon, B. C.; Colpa, J. P. *Can. J. Chem.* **1979**, *57*, 999.
- (8) Buncel, E.; Menon, B. *J. Org. Chem.* **1979**, *44*, 317.
- (9) O'Brien, D. H.; Russell, C. R.; Hart, A. J. *J. Am. Chem. Soc.* **1979**, *101*, 633.
- (10) Grutzner, J. B.; Lawlor, J. M.; Jackman, L. M. *J. Am. Chem. Soc.* **1972**, *94*, 2306.
- (11) Takaki, U.; Hogen-Esch, T. E.; Smid, J. *J. Phys. Chem.* **1972**, *76*, 2152.
- (12) Smid, J. In *Ions and Ion Pairs in Organic Reactions*; Szwarc, M., Ed.; Wiley-Interscience: New York, 1972; Vol. 1.

- (13) Hogen-Esch, T. E.; Smid, J. *J. Am. Chem. Soc.* **1966**, *88*, 318.
- (14) (a) Solov'yanov, A. A.; Beletskaya, I. P.; Reutov, O. A. *Zh. Org. Khim.* **1983**, *19*, 1822 (Engl. Transl. p 1593). (b) Solov'yanov, A. A.; Karpyuk, A. D.; Beletskaya, I. P.; Reutov, O. A. *Dokl. Akad. Nauk SSSR* **1977**, *237*, 360 (Engl. Transl. p 668). (c) Solov'yanov, A. A.; Shtern, M. M.; Beletskaya, I. P.; Reutov, O. A. *Zh. Org. Khim.* **1983**, *19*, 1835 (Engl. Transl. p 1604). (d) Solov'yanov, A. A.; Beletskaya, I. P.; Reutov, O. A. *Zh. Org. Khim.* **1983**, *19*, 1840 (Engl. Transl. p 1608). (e) Solov'yanov, A. A.; Shtern, M. M.; Beletskaya, I. P.; Reutov, O. A. *Izv. Akad. Nauk SSSR, Ser. Khim.* **1982**, *7*, 1673 (Engl. Transl. p 1493). (f) Solov'yanov, A. A.; Karpyuk, A. D.; Beletskaya, I. P.; Reutov, O. A. *Dokl. Akad. Nauk SSSR* **1982**, *262*, 116 (Engl. Transl. p 10). (g) Solov'yanov, A. A.; Dem'yanov, P. I.; Beletskaya, I. P.; Reutov, O. A. *Izv. Akad. Nauk SSSR, Ser. Khim.* **1975**, *10*, 2363 (Engl. Transl. p 2251).
- (15) Petrov, E. S.; Terekhova, M. I.; Lebedeva, T. I.; Basmanova, V. M.; Shatenshtein, A. I. *Zh. Obshch. Khim.* **1978**, *48*, 616 (Engl. Transl. p 561).
- (16) (a) Ellingsen, T.; Smid, J. *J. Phys. Chem.* **1969**, *73*, 2712. (b) Chan, L. L.; Smid, J. *J. Phys. Chem.* **1972**, *76*, 695.